BL-28A/2021S2-001
BL-2A/2022G652

μ-ARPES imaging of polar surface of kagome superconductor CsV_3Sb_5

Takemi KATO[1], Yongkai LI[2,3], Kosuke NAKAYAMA[1,4,*], Zhiwei WANG[2,3], Seigo SOUMA[5,6], Miho KITAMURA[7], Koji HORIBA[8], Hiroshi KUMIGASHIRA[9], Takashi TAKAHASHI[1,5,6] and Takafumi SATO[1,5,6,11,**]

[1]Department of Physics, Graduate School of Science, Tohoku University, Sendai 980-8578, Japan
[2]Centre for Quantum Physics, Key Laboratory of Advanced Optoelectronic Quantum Architecture and Measurement (MOE), School of Physics, Beijing Institute of Technology, Beijing 100081, China
[3]Beijing Key Lab of Nanophotonics and Ultrafine Optoelectronic Systems, Beijing Institute of Technology, Beijing 100081, China
[4]Precursory Research for Embryonic Science and Technology (PRESTO), Japan Science and Technology Agency (JST), Tokyo 102-0076, Japan
[5]Center for Science and Innovation in Spintronics, Tohoku University, Sendai 980-8577, Japan
[6]Advanced Institute for Materials Research (WPI-AIMR), Tohoku University, Sendai 980-8577, Japan
[7]Institute of Materials Structure Science, High Energy Accelerator Research Organization (KEK), Tsukuba, Ibaraki 305-0801, Japan
[8]National Institutes for Quantum Science and Technology (QST), Sendai 980-8579, Japan
[9]Institute of Multidisciplinary Research for Advanced Materials (IMRAM), Tohoku University, Sendai 980-8577, Japan
[10]International Center for Synchrotron Radiation Innovation Smart, Tohoku University, Sendai 980-8577, Japan

1 Introduction

CsV_3Sb_5 is a member of kagome metals AV_3Sb_5 (A = K, Rb, and Cs) which were recently discovered to show superconductivity with T_c = 0.9–2.5 K coexisting with charge density wave (CDW) below T_{CDW} = 78–103 K [1–3] with the in-plane 2×2 periodicity [4–11]. The crystal structure of CsV_3Sb_5 consists of two building blocks, a Cs layer, and a V_3Sb_5 layer, and the cleaved surface is expected to be terminated either by the Cs or V_3Sb_5 (Sb2) layer. Although the bonding between V and Sb1/Sb2 atoms within the V_3Sb_5 layer may be intermetallic, the coupling between the Cs and V_3Sb_5 layers is ionic because Cs is fully ionized (Cs^{1+}) to donate one electron to the V_3Sb_5 layer [$(V_3Sb_5)^{1-}$]. Such ionicity would lead to polar instability. In fact, two different surface terminations have been identified by scanning-tunneling-microscopy (STM) measurements, and intriguingly, there is growing experimental evidence that such a surface hosts peculiar quantum states distinct from those of the bulk as exemplified by the formation of unidirectional 4×1 CDW [4,6–12], surface- dependent vortex-core states [7], and the pair-density wave [4]. However, the band structure associated with the polar surface remains totally unexplored in AV_3Sb_5.

Here, we report a spatially resolved ARPES study of CsV_3Sb_5. By utilizing the microfocused photon beam from the synchrotron[13], we have succeeded in separately observing two kinds of polar surfaces and uncovered marked differences in the band structures between them. The Cs-terminated surface shows the band doubling associated with the three-dimensional (3D) nature of CDW at low temperatures, whereas the Sb- terminated surface is strongly hole doped, resulting in the suppression of CDW. We discuss implications of the present results in relation to the mechanism of the CDW and unconventional surface properties [14].

2 Experiment

High-quality single crystals of CsV_3Sb_5 were synthesized with the self-flux method. ARPES measurements were performed using Scienta-Omicron DA30 and SES2002 spectrometers at BL-28A and BL-2A in Photon Factory, KEK. We used energy tunable photons of $h\nu$ = 85–350 eV. ARPES data were mainly obtained by circularly polarized 106-eV photons (corresponding to the out-of-plane wave vector $k_z \sim 0$) with the beam spot size of 10×12 μm^2 [13]. The energy resolution was set to be 25 meV. The samples were cleaved at the same temperatures at which the ARPES measurements were performed (8 and 120 K). All the data have been recorded within 8 hs after the cleavages.

3 Results and Discussion

Figure 1(a) shows a mapping of the spatial distribution of the binding energy (E_B) of Sb-4$d_{5/2}$ core-level peak [see Fig. 1(c)] by sweeping the microfocused photon beam on the surface of CVS. This is a good measure of the surface doping level (note that the selection of the Sb-4$d_{3/2}$ peak reproduces the same result). As seen in Fig. 1(a), the surface looks to consist of two regions (blue and red regions). The core-level spectrum in the red region [red curve in Fig. 1(c)] is shifted as a whole toward higher E_B by ~130 meV with respect to that in the blue region (blue curve), indicating that the red region is more electron

doped than the blue region. Such a difference in the doping level signifies different polarities of the two regions. Here we assign the electron (hole)-rich red (blue) region to the Cs (Sb)-terminated surface because Cs atoms on top surface do not need to donate electrons to the missing upper V_3Sb_5 layer which is removed by the cleaving so that the V_3Sb_5 layer beneath the topmost Cs layer is more electron doped for the Cs-terminated surface. Inversely, the V_3Sb_5 layer at the surface is hole doped compared with the bulk counterpart. This is also corroborated by the behavior of the Cs-4*d* core level. Figure 1(d) shows the Cs-4*d* core-level spectra measured at the same spatial location as in Fig. 1(b) where we observe that each spin-orbit satellite of Cs-4*d* core levels ($d_{5/2}$ or $d_{3/2}$) consists of two peaks; a peak at lower E_B originates from bulk Cs atoms whereas that at higher E_B is from surface Cs atoms as confirmed by the angular dependence of their intensity ratio. One can recognize that the surface Cs peak is stronger than the bulk one for the Cs-termination-dominant surface (red curve), whereas it is weaker for the Sb-termination-dominant case (blue curve). The spatial image of the intensity ratio between the surface and the bulk Cs peaks in Fig. 1(b) shows good agreement with that of the Sb-core-level E_B in Fig. 1(a). This supports our assignment of the Cs- and Sb-termination-dominant surfaces (hereafter, we simply call them Cs- and Sb-terminated surfaces, respectively) as schematically shown in Fig. 1(e).

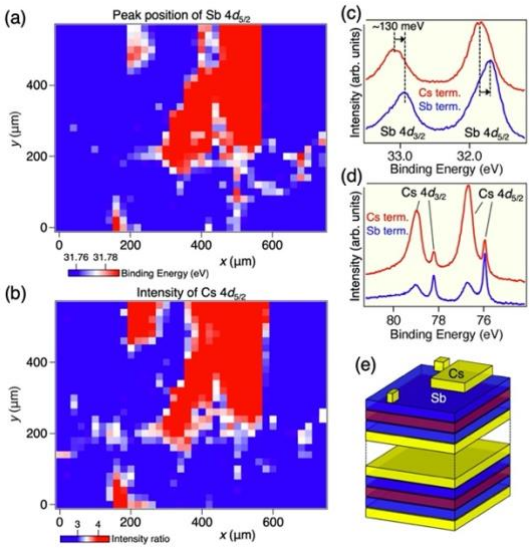

Fig. 1 (a) Spatial map of the E_B position of Sb-4d$_{5/2}$ core level measured with $h\nu$ = 106 eV at T = 8 K in the spatial region enclosed by red dashed rectangle (area size: 600×800 μm^2), obtained with the step size of 20 μm. (b) Spatial map of the intensity ratio of the surface/bulk Cs-4d$_{5/2}$ core-level peaks. (c) and (d) EDC in the Sb-4*d* and Cs-4*d* core-level regions, respectively, for the Cs-(red) and Sb-(blue) terminated surfaces. (e) Schematic of the cleaved surface of CsV_3Sb_5.

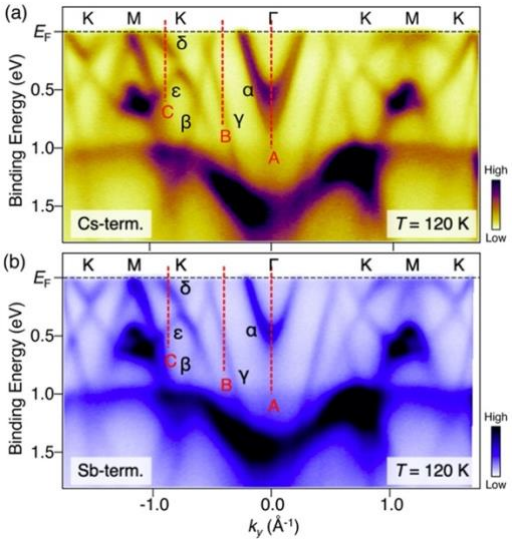

Fig. 2 (a) and (b) ARPES intensity at T = 120 K for Cs- and Sb-terminated surfaces, respectively, measured with $h\nu$ = 106 eV along the ΓKM cut.

Figs. 2(a) and 2(b) show the ARPES intensity at T =120K (above T_{CDW} =93K) along the ΓKM cut (k_z ~0) for the Cs- and Sb-terminated surfaces, respectively. One can recognize overall similarity in the band structure between the two, i.e., an electron band at the Γ point (α) with the Sb-5p_z character, linearly dispersive V-3$d_{xz/yz}$ bands (β, γ) forming a Dirac cone near E_F (marked by an arrow), the δ band with the V-3$d_{xy/x2-y2}$ character forming a saddle point (SP) slightly above E_F, and the ε band that intersects the δ band to form a Dirac point at the K point at EB ~ 0.3 eV. A closer look further reveals some intrinsic differences; the band structure of the Cs-terminated surface is shifted downward as a whole with respect to that of the Sb-terminated surface as recognized by a direct comparison of surface-termination-dependent ARPES spectra at representative k points along cut A-C in Figs. 2(a) and 2(b). Numerical fittings to the peak position clarified the energy shift to be 30–90 meV (note that a finite variation in the magnitude of the energy shift among different bands and Sb-4d core levels suggests a non-rigid-band-type energy shift. Moreover, whereas the Sb-terminated surface exhibits a single α band bottomed at EB ~ 0.5 eV, it splits into two bands bottomed at E_B ~ 0.5 and 0.8 eV for the Cs-terminated surface. This suggests that not only polarity, but also the band structure above T_{CDW} is different between the Cs- and the Sb-terminated surfaces. We have performed ARPES measurements more than three times with different samples for each surface termination and confirmed the reproducibility.

We further measured temperature dependence of ARPES data across T_{CDW} and examined its termination dependence [14]. We found that the Cs-terminated surface shows intriguing doubling of V-derived bands at low temperatures associated with the band folding due to the three-dimensional CDW, whereas the Sb-terminated one shows no band doubling or resultant CDW-gap opening indicative of the suppression of bulk-originated CDW due to polar charge. Such polar-surface-dependent band

structures must be incorporated for understanding the origin of unconventional superconducting and charge order at the surface of AV_3Sb_5 [14].

Acknowledgements

This work was supported by JST-CREST (No. JPMJCR18T1), JST-PREST (No. JPMJPR18L7), JSPS KAKENHI Grants (No. JP21H04435 and No. JP20H01847). T. K. acknowledges support from GP-Spin at Tohoku University.

References

[1] B. R. Ortiz, L. C. Gomes, J. R. Morey, M. Winiarski, M. Bordelon, J. S. Mangum, I. W. H. Oswald, J. A. Rodriguez-Rivera, J. R. Neilson, S. D. Wilson, E. Ertekin, T,M. McQueen, and E. S. Toberer, Phys. Rev. Mater. **3**, 3094407 (2019).

[2] B. R. Ortiz, S. M. L. Teicher, Y. Hu, J. L. Zuo, P. M. Sarte, E.C. Schueller, A.M.M. Abeykoon, M.J. Krogstad, S. Rosenkranz, R. Osborn, R. Seshadri, L. Balents, J. He, and S. D. Wilson, Phys. Rev. Lett. **125**, 247002 (2020).

[3] Q. Yin, Z. Tu, C. Gong, Y. Fu, S. Yan, and H. Lei, Chin. Phys. Lett. **38**, 037403 (2021).

[4] H. Chen, H. Yang, B. Hu, Z. Zhao, J. Yuan, Y. Xing, G. Qian, Z. Huang, G. Li, Y. Ye et al., Nature (London) **599**, 222 (2021).

[5] Y.-X. Jiang *et al*., Nat. Mater. **20**, 1353 (2021).

[6] H. Zhao, H. Li, B. R. Ortiz, S. M. L. Teicher, T. Park, M. Ye, Z. Wang, L. Balents, S. D. Wilson, and I. Zeljkovic, Nature (London) **599**, 216 (2021).

[7] Z. Liang, X. Hou, F. Zhang, W. Ma, P. Wu, Z. Zhang, F. Yu, J.-J. Ying, K. Jiang, L. Shan, Z. Wang, and X.-H. Chen, Phys. Rev. X **11**, 031026 (2021).

[8] Z. Wang, Y.-X. Jiang, J.-X. Yin, Y. Li, G.-Y. Wang, H.-L. Huang, S. Shao, J. Liu, P. Zhu, N. Shumiya, M. S. Hossain, H. Liu, Y. Shi, J. Duan, X. Li, G. Chang, P. Dai, Z. Ye, G. Xu, Y. Wang et al., Phys. Rev. B **104**, 075148 (2021).

[9] N. Shumiya, M. S. Hossain, J.-X. Yin, Y.-X. Jiang, B. R. Ortiz, H. Liu, Y. Shi, Q. Yin, H. Lei, S. S. Zhang, G. Chang, Q. Zhang, T. A. Cochran, D. Multer, M. Litskevich, Z.-J. Cheng, X. P. Yang, Z. Guguchia, S. D. Wilson, and M. Z. Hasan, Phys. Rev. B **104**, 035131 (2021).

[10] L. Nie, K. Sun, W. Ma, D. Song, L. Zheng, Z. Liang, P. Wu, F. Yu, J. Li, M. Shan, D. Zhao, S. Li, B. Kang, Z. Wu, Y. Zhou, K. Liu, Z. Xiang, J. Ying, Z. Wang, T. Wu et al., Nature (London) **604**, 59 (2022).

[11] H. Li, T. T. Zhang, T. Yilmaz, Y. Y. Pai, C. E. Marvinney, A. Said, Q. W. Yin, C. S. Gong, Z. J. Tu, E. Vescovo, C. S. Nelson, R. G. Moore, S. Murakami, H. C. Lei, H. N. Lee, B. J. Lawrie, and H. Miao, Phys. Rev. X **11**, 031050 (2021).

[12] H.-S. Xu, Y.-J. Yan, R. Yin, W. Xia, S. Fang, Z. Chen, Y. Li, W. Yang, Y. Guo, and D.-L. Feng, Phys. Rev. Lett. **127**, 187004 (2021).

[13] M. Kitamura, S. Souma, A. Honma, D. Wakabayashi, H. Tanaka, A.Toyoshima, K. Amemiya, T. Kawakami, K. Sugawara, K. Nakayama, K. Yoshimatsu, H. Kumigashira, T. Sato, and K. Horiba, Rev. Sci. Instrum. **93**, 033906 (2022).

[14] T. Kato, Y. Li, K. Nakayama, Z. Wang, S. Souma, M. Kitamura, K. Horiba, H. Kumigashira, T. Takahashi, and T. Sato, Phys. Rev. B **106**, L121112 (2022).

* k.nakayama@arpes.phys.tohoku.ac.jp
** t-sato@arpes.phys.tohoku.ac.jp